P4A.2

DOPPLER-RADAR OBSERVATIONS OF DUST DEVILS IN TEXAS

Howard B. Bluestein* and Christopher C. Weiss
University of Oklahoma
Norman, Oklahoma

Andrew L. Pazmany
University of Massachusetts
Amherst, Massachusetts

1. INTRODUCTION

Most of what we know about the observed structure and behavior of dust devils comes from in situ ground-based and airborne measurements (e.g., Sinclair 1973). These measurements have provided, at best, a look at one-dimensional slices through dust-devil vortices.

A W-band (3-mm wavelength), truck-mounted pulsed Doppler radar system designed and developed at the Univ. of Mass. at Amherst has been used at the Univ. of Oklahoma during the spring of recent years to probe tornadoes and other convective phenomena in the plains of the U. S. (Bluestein and Pazmany 2000).

The purpose of this paper is to describe a dataset collected in several dust devils near Tell, TX, southwest of Childress, during the afternoon of 25 May 1999. This dataset improves on the overall coverage and both spatial and temporal resolution of prior dust-devil datasets consisting only of in situ measurements.

2. DESCRIPTION OF THE RADAR

The W-band radar antenna has a half-power beamwidth of 0.18^{o} and a range resolution of 15 m (pulse length is increased from 15 m to 30 m to enhance the sensitivity over what is necessary to probe tornadoes), so that very high-resolution velocity and reflectivity data can be obtained at close range in small-scale, boundary-layer vortices. At the ranges of the dust devils to be discussed, the azimuthal resolution ranged from 3 m to 5 m.

Sector scans were obtained to the southeast at low elevation angle (as close to the ground as was possible) every 5-13 s, depending on how wide the scans were. The width of the scans was wider than the width of the visible dust column of the dust devils. A boresighted video camera was used to aim the antenna.

It is thought that the backscattered signal received at the radar was from insects (in clear air) and airborne dust particles. The signal was likely in most part due to Mie scattering.

The pulse-repetition frequency was such that the maximum unambiguous velocity was ±8 m s^{-1}. For some dust devils, the velocity data were aliased, but were easily corrected.

3. RESULTS

Four dust devils (A-D) were probed at ranges of 900 m to 1.5 km. Three (A-C) were cyclonic and one (D) was anticyclonic.

a. Radar depiction of cyclonic and anticyclonic dust devils

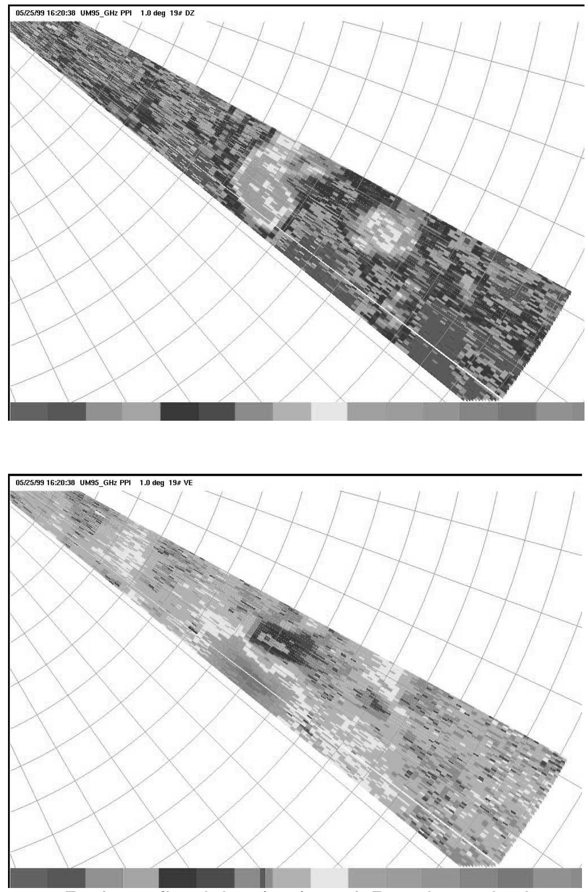

Figure 1. Radar reflectivity (top) and Doppler velocity (bottom) at the lowest elevation angle possible at 1520:38 CDT on 25 May 1999, just west of Tell, TX. Constant-range rings are plotted at 100-m increments; constant-azimuth spokes are plotted at 5° increments. Gray scales for each panel range from –30 dBZe at far left to 0 dBZe at far right (top panel) and –10 m s^{-1} at far left to +15 m s^{-1} at far right (bottom panel). Dust devil to left (B) is cyclonic; small dust devil to right (D) is anticyclonic.

The radar reflectivity signature of the dust devils was frequently a quasi-circular ring of enhanced backscatter surrounding a weaker-echo eye (Fig. 1), similar to the reflectivity structure of tornadoes (e.g., Bluestein and Pazmany (2000)). It is thought that the ring is caused by the dust/debris encircling the dust devil vortex. The associated Doppler-velocity pattern with each dusts devil was that of a vortex signature.

* Corresponding author address: Howard B. Bluestein, School of Meteorology, University of Oklahoma, Norman,OK 73019; e-mail: hblue@ou.edu

The diameters of the cores (distance across the maxima-minima Doppler-velocity couplet) of these Texas-sized dust devils ranged from 30 – 130 m, which are much wider than that of typical dust devils in a homogeneous environment. Maximum ground-relative wind speeds in each dust devil ranged from 6.5 – 13.5 m s^{-1}.

b. Dust-devil interaction

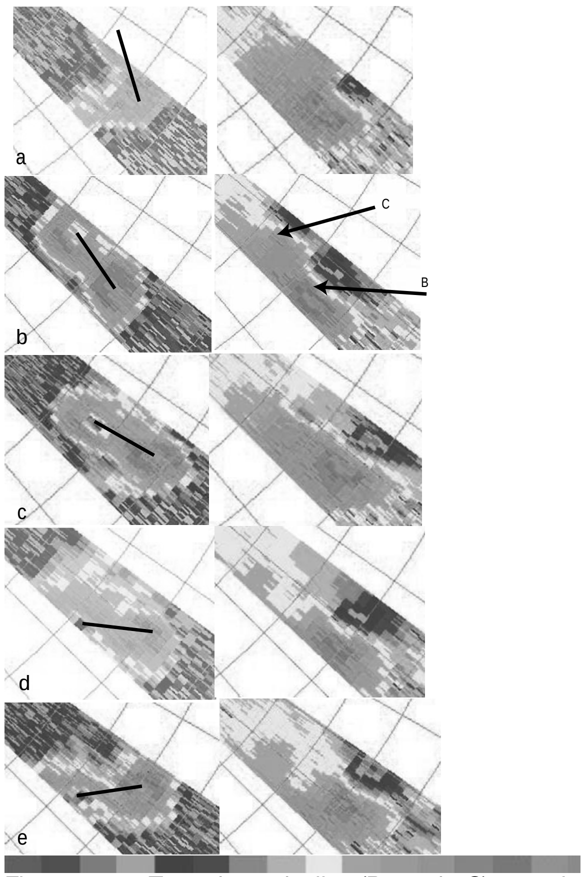

Figure 2. Two dust devils (B and C) rotating cyclonically around each other. As in Fig. 1, but at (a) 1518:07, (b) 1518:16, (c) 1518:23, (d) 1518:32, and (e) 1518:39 CDT. Panel on left (right) is for radar reflectivity (Doppler velocity). A line connecting the approximate center of the two vortices is shown (left panels) to aid the reader in visualizing the rotation of each vortex about the other. In (a), the center of the vortex C was extrapolated subjectively. Arrows are shown to distinguish between the signatures of dust devils B and C in (b) only.

Two adjacent dust devils (B and C) were noted rotating cyclonically around each other during a 32-s interval (Fig. 2). It appeared that B was the primary one, while C appeared serendipitously at the edge of the 1518:07 CDT (all times given in CDT) scan, and passed out from the edge of the scan after 1518:39. The dust devils B and C behaved according to the Fujiwhara effect (e. g., Fujiwhara 1931), through which vorticity from each one is advected by the wind field from the other.

c. Radial profiles of reflectivity, Doppler velocity, vorticity, and divergence

To estimate the azimuthal and radial wind components, vertical vorticity, and horizontal divergence in the dust devils, it was necessary to assume that to a first approximation, the dust-devil vortices were circularly symmetric. The radial profiles of azimuthal-wind component were estimated from the Doppler velocities at the ranges of the centers of the dust devils as a function of azimuth; the radial profiles of radial-wind component were estimated from the Doppler velocities at the azimuths of the centers of the dust devils, as a function of range. The Doppler wind data at adjacent ranges and azimuths were also inspected subjectively to ensure that the centers of the dust-devil vortices were correctly located. Vorticity (divergence) was estimated in polar coordinates from the azimuthal- (radial-) wind component profiles.

Vortex motion was estimated, so that the vortex-relative wind components could be computed. In addition, each profile of ground-relative azimuthal wind was adjusted so that the azimuthal wind component at the center was as close to zero as possible and so that the maxima in azimuthal wind component of the near and far sides of each vortex were approximately equal. It was not always possible to satisfy both of these conditions exactly, most likely because the vortices were not precisely circularly symmetric (i.e., there was multiple-vortex structure). Both the latter procedure and simple tracking of the location of dust devils A and

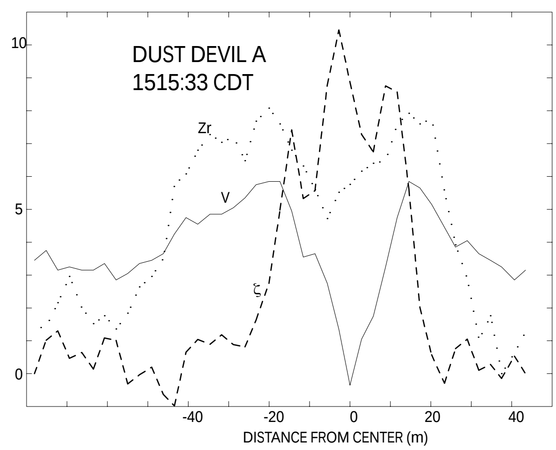

Figure 3. Approximate vortex-relative azimuthal wind component V (solid line; m s^{-1}), vorticity ζ (dashed line: X 10 s^{-1}), and the relative radar reflectivity $Zr = (Z - Z_{noise})/C$, where Z is the radar reflectivity factor (dBZ), Z_{noise} (dBZ) a subjectively determined approximate noise floor, and C is dimensionless compression factor chosen subjectively so that the range of relative reflectivity remains within the scale of the figure, in dust devil A, at 1515:33 CDT, as a function of distance from the center of the vortex (m); negative (positive) distances are measured to the left (right) of the vortex center, as viewed by the radar. The vorticity at the center is estimated as the average of the vorticities computed just to the right and left of the center.

B yielded an along-the-beam motion of around 2.3 – 3.2 m s^{-1} away from the radar. The wind experienced at the radar was light and from the northwest, while the dust devils propagated to the southeast.

The radial profile of dust-devil relative azimuthal wind in dust devil A, at 1515:33 was like that of a Rankine-combined vortex (Fig. 3). The vortex had a core of vorticity of 0.7 – 1 s^{-1} and approximately solid-body rotation, surrounded by potential flow. The vorticity (O(1 s^{-1})) is as high as it is in some tornadoes (Wurman and Gill 2000), because relatively small changes in azimuthal wind speed are found at correspondingly small changes in radial distance. A ring of maximum radar reflectivity was coincident with the radius of maximum azimuthal wind (RMW).

The radial profile of dust-devil relative radial wind was composed of very small wind speeds and therefore not reliable: The radial distribution of divergence exhibited no symmetry about the dust-devil vortex (not shown).

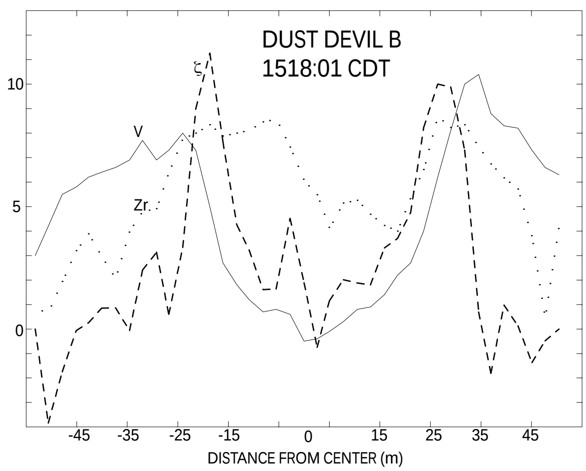

Figure 4. As in Fig. 3, but for dust devil B at 1518:01 CDT, when it was most intense.

The structure of dust devil B (Figs. 4 and 5) was significantly different from that of dust devil A. A's RMW was more than twice as wide (~ 35 m rather than 15 m) at 1518:01 (Fig. 4), when the dust-devil vortex of B was producing the strongest ground-relative wind speeds of 13.6 m s^{-1}. Rather than behaving like a Rankine-combined vortex, it had a 10-15–m wide annulus of strong shear vorticity just inside the RMW. The center of the vortex had an eye of relative calm, approximately 40 m in diameter; outside the annulus of vorticity there was approximate potential flow. The radar reflectivity profile had a broad, weak-echo eye; there was a ring of high reflectivity within the RMW, not coincident with it as in dust devil A.

The radial profile of dust-devil relative wind (Fig. 6), that corresponded to the azimuthal-wind profile seen in Fig. 5, exhibited a relatively high degree of symmetry about the center (compared to that at other times). Inside the eye, just above the ground, a 30-m wide zone of convergence near the center, was surrounded by a ring of convergence located about 70-80 m from the center. It is therefore inferred kinematically that

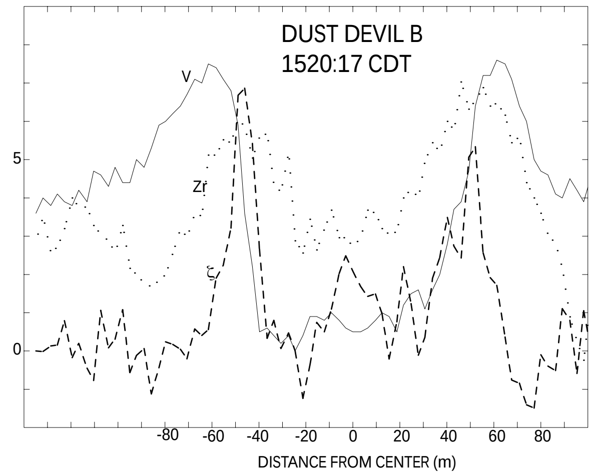

Figure 5. As in Fig. 3, but for dust devil B, several minutes later at 1520:17 CDT, when the reflectivity ring had the most circular appearance.

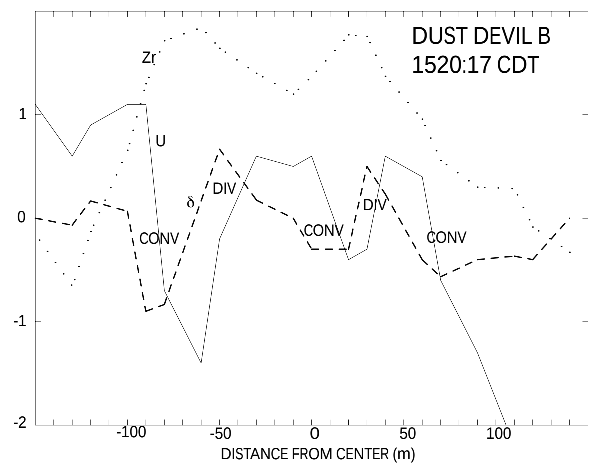

Figure 6. Approximate vortex-relative radial wind component (solid line; m s^{-1}), horizontal divergence (dashed line; X 10 s^{-1}), and relative radar reflectivity factor as in Fig. 3, as a function of distance from the center of the vortex (m); negative (positive) distances are measured within (beyond) the vortex center. Prominent regions of divergence (δ>0) and convergence (δ<0) around the vortex are noted.

the broad eye was characterized by sinking motion and that the area near the RMW was characterized by rising motion: Such a structure is two-celled. At this time, when the highest degree of circular symmetry is seen and the radial profile of radial wind can be accepted with the highest degree of confidence, the centers of the regions of convergence surrounding the dust devil are located beyond the RMW. It thus appears that the width of the dust devil, which was increasing with time (not shown), may have been doing so because the annulus of vorticity was propagating radially outward: Low-level convergence acting on the outer portion of the annulus would tend to propagate the annulus radially outward. To test the viability of this hypothesis, radial wind profiles just before and after this scan were inspected. At the time of the preceding and subsequent scans, the radial-wind profiles (not shown) lacked sufficient symmetry to be acceptable. At the time of the last scan, over a minute later, there was still a lack of symmetry; by this time, the RMW ceased increasing. The hypothesis can therefore not be evaluated; it is likely that asymmetries due to multiple vortex structure rendered the procedure of estimating the radial profile of radial wind component inaccurate.

c. Evidence of Rossby-like wave motion

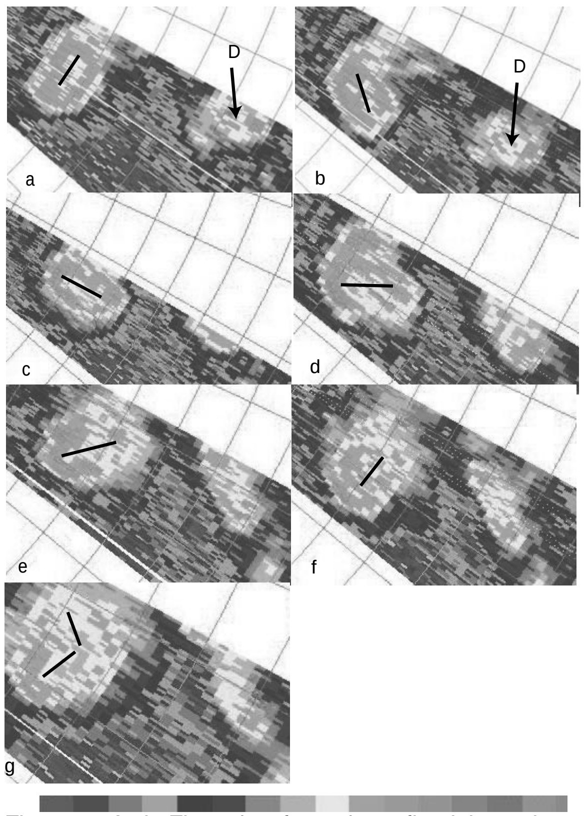

Figure 7. As in Fig. 2, but for radar reflectivity only at (a) 1520:26, (b) 1520:38, (c) 1520:52, (d) 1521:01, (e) 1521:10, (f) 1521:20, and (g) 1521:30. A line aligned approximately along the major axis of the elliptical reflectivity ring associated with dust devil B is shown to help the reader visualize how it rotated from scan to scan. In (g) two conjoined ellipses are noted.

The major axis of the reflectivity ring associated with dust devil B rotated cyclonically about its center one revolution in approximately 60 s. The angular speed of rotation is consistent with that of a Rossby-like wave in a Rankine vortex (core vorticity/4) whose core has vorticity $\sim 0.5\ s^{-1}$ (Lamb 1945). It is not clear, however, to what extent Lamb's theory can be applied to dust devil B, which was not a Rankine-combined vortex.

4. CONCLUDING COMMENTS

The mobile, W-band radar, with its very narrow beam, was able to resolve the structure of very wide dust devils at close range. Structure similar to that seen in numerical and laboratory simulations of tornado-like vortices was found (e.g., cf. Fig. 5.29 in Davies-Jones et al. 2001): It is speculated that the structure of dust devil A is consistent with that of a low-swirl-ratio vortex, while the behavior of dust devil B is consistent with that of a high-swirl ratio vortex.

It was surprising that the maximum in radar reflectivity was so often located within the RMW. Bluestein et al. (2003) found that in a tornado vortex the maximum in reflectivity at low levels was also inside the RMW. It is speculated that dust particles are transported radially inward within the RMW in the surface layer (Dowell 2003; personal communication).

It is suggested that future explorations include an investigation of the mechanisms for the formation of dust devils. To do so, it will be necessary to scan much wider segments so that the clear-air boundary-layer flow can be resolved over a broad area, prior to vortex formation. In addition, the signal-processing unit of the radar needs to be upgraded to allow for more rapid data collection.

ACKNOWLEDGMENTS

This research was funded by National Science Foundation (NSF) grants ATM- 9912097 at the Univ. of Okla. and ATM-9616730 at U. Mass. It was completed while the first author was on sabbatical leave at the National Center for Atmospheric Research (NCAR) in the Mesoscale and Microscale Meteorology Division. NCAR is supported by the NSF. Jose Castilleja, Pat Waukau, Jody Williams, Kris Conrad, and David Dowell provided valuable computer-related and graphics-related assistance.

REFERENCES

Bluestein, H. B., W.-C. Lee, M. Bell, C. C. Weiss, and A. L. Pazmany, 2003: Mobile-Doppler radar observations of a tornado in a supercell near Bassett, Nebraska on 5 June 1999. Part II: Tornado-vortex structure. Mon. Wea. Rev. (in review)

Bluestein, H., and A. L. Pazmany, 2000: Observations of tornadoes and other convective phenomena with a mobile, 3-mm wavelength, Doppler radar: The spring 1999 field experiment. Bull. Amer. Meteor. Soc., **81**, 2939-2951.

Davies-Jones, R., R. J. Trapp, and H. B. Bluestein, 2001: Tornadoes and tornadic storms (Chap. 5). Severe Convective Storms, Amer. Meteor. Mongraph. No. 50, **28**, 167-221.

Fujiwhara, S., 1931: Short note on the behavior of two vortices. Proc. Phys.-Math. Soc. Japan, Ser. 3, **13**, 106-110.

Lamb, H. , 1945: Hydrodynamics. Dover, 738 pp.

Sinclair, P. C., 1973: The lower structure of dust devils. J. Atmos. Sci., **30**, 1599-1619.

Wurman, J., and S. Gill 2000: Finescale radar observations of the Dimmitt, Texas (2 June 1995), tornado. Mon. Wea. Rev., **128**, 2135-2164.